A miniaturized printed rectenna for wireless RF energy harvesting around 2.45 GHz

Mohsen Koohestani, Jérôme Tissier, Mohamed Latrach

Version of Record: https://www.sciencedirect.com/science/article/pii/S1434841120314795
Manuscript_7e6328a853a800a4c9ccdc3c0656c68f

A miniaturized printed rectenna for wireless RF energy harvesting around 2.45 GHz

Mohsen Koohestani[a,b], Jérôme Tissier[a,b], Mohamed Latrach[a,b]

[a] *École Supérieure d'Électronique de l'Ouest (ESEO), Department of Electrical and Control Engineering, 49107 Angers, France*
[b] *Institute of Electronics and Telecommunications of Rennes (IETR), University of Rennes 1, 35042 Rennes, France*

Abstract

This paper presents the design of a highly compact printed rectenna for ambient RF energy harvesting around 2.45 GHz. Its antenna structure comprises a rectangular patch with two etched U-shaped slots fed by a symmetric 50 Ω coplanar line. In spite of compact size, it has been directly integrated with a rectifying circuit on the same substrate only at the expense of a 15% frequency shift. The proposed rectenna overall dimension is only $24.9 \times 8.6 \times 1.6\ mm^3$, the smallest so far reported with comparable performance, which can be easily integrated with any device for energizing low-power wireless sensor networks. It was fabricated and experimentally characterized, achieving a reasonable agreement with the expected simulated results. Measured results indicate that, at the resonant frequency, the antenna part of the proposed rectenna provides a good matching level (< -25 dB) and has a 0.8 dBi peak gain as well as nearly symmetrical radiation properties (in both E- and H-planes). The measured RF-to-DC conversion efficiency (DC output voltage) of the proposed rectenna at a low incident power of −20 dBm is about 20% (97 mV) with a load resistance of 4.7 kΩ. A demonstration experiment of a LED driven by the rectenna was also presented.

Keywords: Wireless energy harvesting, rectenna, compact design, symmetric CPW-fed, power conversion efficiency

*Corresponding author: Mohsen Koohestani (mohsen.koohestani@eseo.fr)

1. Introduction

Radio frequency (RF) energy harvesting, also referred to as RF energy scavenging, has recently become one of the most favorable technology to energize low power electronic devices from the large amount of ubiquitous electromagnetic energy in atmosphere (e.g. TV and radio broadcastings, wireless LAN, and mobile phone signals) [1]. This potentially lowers the cost of a system by eliminating the need for batteries and/or power supply resources, which comes in very handy, for instance, in wireless monitoring systems embedded in the concrete that are not directly accessible for battery replacement [2]. The rectifying antenna (so called rectenna) is the key component of RF energy harvester having an almost unlimited lifetime (unlike batteries). Moreover, in an increasingly mobile world with human being attached to electronic gadgets, from a safety and health point of view, exposure to rectennas is most likely harmless [3].

A typical rectifying circuit, which converts the wireless RF energy to DC power, comprises either CMOS- or Schottky-based diodes. The latter is usually preferred due to potentially lower threshold voltage and larger power handling capabilities [4]. In order to maximize the energy transfer between the receiving antenna and the rectifying circuit, a matching circuit has to be designed [1, 4]. The commonly used approaches to enhance power conversion efficiency (PCE) include optimizing the input matching by source pull technique [5], designing antenna arrays [6] or antennas with harmonic rejection properties [7], and increasing the input power [8].

In a rectenna, the antenna part, which usually occupies a larger area compared to the rectifying circuit, plays an important role in capturing power, acting as a transducer between propagating and guided waves. In a modern wireless world with compact electronic devices, the design of an antenna having a small size is a challenging task and of high demand. Among various antenna types, printed antennas are highly desired due to their low profile, light weight, low cost, ease of fabrication, and the ability to easily integrate with the rectifying circuit. With the rapid development of printed technology, various antenna types have

been designed with many various shaped radiators, such as diamond, rectangular, fractal, circular, and crescent geometries for narrow- and wide-band wireless applications [9–16]. The most commonly used techniques to reduce antenna size are employing asymmetric excitation [16], creating slots/slits on the antenna radiating elements [17], sandwich loading [18] and corrugating the antenna [19].

The choice of the operating frequency is also an important consideration in RF energy harvesters. In order to avoid oversized devices and difficulty in installation, the 2.45 GHz industrial, scientific, and medical (ISM) band can be considered a suitable option, as it offers a good trade-off among the signal attenuation, antenna size and frequency. It is worth mentioning that, for energy harvesting applications, a multiple-band rather than a wideband antenna is preferred due to the RF-to-DC diode input impedance changing with frequency, as well as the impracticality to design a wideband matching circuit using several lumped components (bulky and lossy) to adapt the diode impedance to the one of the antenna [20].

A few compact 2.45 GHz printed antenna designs with various feeding structures are reported in literature; microstrip (MS)-fed [10, 13], coplanar waveguied (CPW)-fed [11, 12], and asymmetric coplanar strip (ACS-fed) [14–16]. Table 1 provides a summary of state-of-the-art antenna designs comparing their structure, size and peak gain at resonance. Note that although ACS-fed antennas are generally smaller than symmetric coplanar-fed ones, but due to inherent asymmetry introduced into the antenna they may suffer from asymmetric radiation pattern [16], not being suitable in array configurations, and lead to decreased isolation that can be achieved in MIMO applications [21]. Here, in order to end up with a compact rectenna design, a very compact printed antenna is proposed, which benefits from a symmetric feeding structure with an overall size of 24.9 mm $\times$ 8.6 mm, about 10.8% less area than the smallest so far reported [16] while operating even at a 5.8% lower frequency.

Regarding the compact printed rectenna designs operating at 2.45 GHz [22–28], Table 2 provides a summary of state-of-the-art rectenna designs comparing their size and RF-to-DC efficiency with respect to input power and load value. Here, a matched voltage doubler

Table 1: State-of-the-art design of printed monopole antennas operating around 2.45 GHz

Ref.	Antenna structure	Dimensions (mm × mm)	Peak gain at resonant frequency
[9]	MS-fed L-shaped monopole	40 × 30	1.0 dBi @ 2.44 GHz
[10]	CPW-fed T-shaped monopole with L-strips	30 × 27	1.3 dBi @ 2.4 GHz
[11]	CPW-fed monopole patch with rectangular slots	30 × 18	5.6 dBi @ 2.45 GHz
[12]	MS-fed monopole with horizontal and spiral strips	32 × 12	1.7 dBi @ 2.5 GHz
[13]	ACS-fed monopole with C-shaped slots	32 × 12	1.0 dBi @ 2.5 GHz
[14]	ACS-fed circular-arc-shaped monopole	22.1 × 12	1.6 dBi @ 2.4 GHz
[15]	ACS-fed meander monopole	24 × 10	1.6 dBi @ 2.6 GHz
This work	CPW-fed monopole patch with rectangular slots	24.9 × 8.6	0.8 dBi @ 2.45 GHz

Table 2: State-of-the-art design of 2.45 GHz rectennas in literature

Ref.	Size (mm × mm)	Area (mm^2)	P_{in} (dBm)	R_L (kΩ)	PCE (%)	PCE* (%)
[21]	78 × 50	3900	10	1	70.2	N/A
[22]	60 × 60	3600	20	1	70.6	N/A
[23]	48 × 48	2304	-10	2.1	31.9	33.47
[24]	50 × 40	2000	-15	10	31.8	29.66
[25]	43.5 × 33.7	1466	0	0.4	21.6	15.5
[26]	34 × 34	1156	-10	5	42.1	40.29
[27]	52 × 20	1040	-15	2.2	30	24.05
This work	24.9 × 8.6	214.1	-20	4.7	20	20

N/A: not applicable, due to diode input power limits used in numerical simulations.
PCE* is the PCE of the proposed rectenna with similar P_{in} and R_L.

(comprising two Schottky diodes in the same package) is embedded in the antenna structure, as a showcase, to further keep its small size while maintaining good performance. As observed, the proposed design has about 79% less area than previously reported rectennas for RF energy harvesting. A fair comparison in terms of PCE with load and input power levels, referred to as PCE* in Table 2, similar to those reported in [24–28] shows that the PCE* values are comparable to those previously achieved by the above-cited rectennas but in a much smaller area; see more details in Section 3.

2. Antenna structure and design

In order to keep the overall rectenna dimensions as compact as possibe, the antenna part, which occupies the most area of a rectenna, has to be possibly small while maintaing the desired performace. Fig. 1 shows the geometry and the design parameters of the proposed

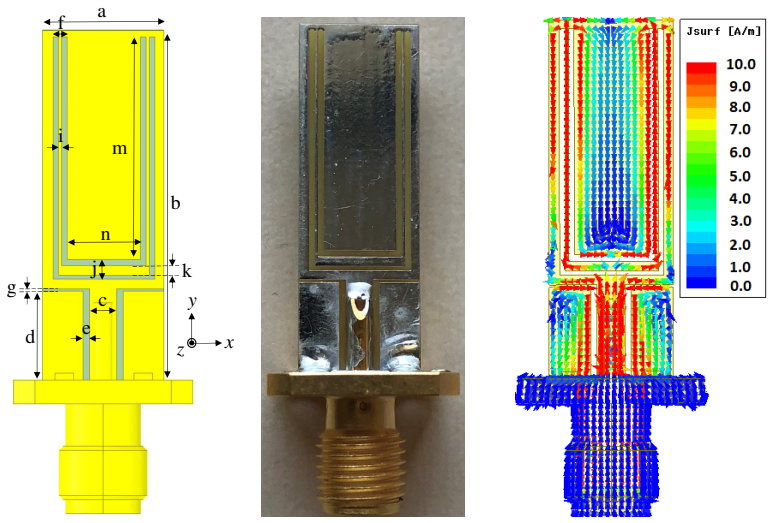

(a) (b) (c)

Figure 1: Proposed antenna (a = 8.6 mm, b = 24.9 mm, c = 2 mm, d = 6.3 mm, e = 0.45 mm, f = 1 mm, g = 0.15 mm, i = 0.2 mm, j = 1.4 mm, k = 0.7 mm, m = 15.8 mm, n = 5.2 mm): (a) geometry, (b) prototype photograph, (c) current distribution at 2.45 GHz.

antenna. The miniaturisation was achieved using a combination of known techniques (i.e. inserting slots on the antenna radiator), however, preserving the compactness of the antenna requires substantial effort and makes the design innovative. The radiating patch comprises a rectangular section including two truncated U-shaped slots. It is fed by a symmetric coplanar line of 2 mm width and 0.45 mm gap. It is printed on an inexpensive FR4 epoxy substrate ($\varepsilon_r = 4.4 \pm 5\%$, $h = 1.6$ mm, and $\tan\delta = 0.02$). The other side of the substrate is devoid of metalization. The area of the fabricated antenna is 24.9×8.6 mm^2 (Fig. 1), being about 10.8% smaller than the one presented in [16] which is the smallest printed antenna so far reported, while operating even at a 5.8% lower frequency.

The performance of the antenna was investigated by Ansys HFSS and its optimized parameters are given in Fig. 1. In order to demonstrate the antenna operation at 2.45 GHz, the current distribution on the antenna is depicted in Fig. 1c. The currents are mostly concentrated around the U-shaped slots and the edge portions of radiating patch and ground, which indicate that those elements mainly affect the performance of the proposed antenna.

In order to further investigate this and to show how the antenna was originally designed, the effects of the key geometrical parameters (e.g. the U-shaped slots dimensions) were

investigated. Note that only one parameter was varied at the time.

The two U-shaped slots on the antenna radiating patch are responsible for two different frequency bands, i.e. the outer slot for 2.1 GHz and the inner one for 2.45 GHz (Fig. 2a). Although the aim here is to design a compact antenna operating at 2.45 GHz, the outer slot which is responsible for the lower frequency in the band, was included in the design as it improves matching at the target frequency bearing also in mind that multi-band antennas are desired for RF energy harvesting [29]. This, however, reduces the antenna gain from 1 to 0.82 dBi due to the current opposition around the two slots (Fig. 1c). It is worth mentioning that, as can be seen in Table 1, comparing the gain of similarly sized antennas developed in [15] (1.6 dBi at 2.45 GHz) and [16] (1.6 dBi at 2.6 GHz) to the proposed one (0.8 dBi at 2.45 GHz), which is smaller by 44.2% and 10.8%, respectively, shows a valid trade-off between antenna size reduction and performance degradation to a reasonable extent.

Figs. 2b to 2d show the antenna input reflection coefficients with respect to the slots dimensions. It can be seen how precisely the antenna resonant frequency and impedance bandwidth can be controlled by tuning 'i','m', and 'k' parameters. From the fabrication point of view, the antenna performance is very sensitive to the variations of those parameters due to its compact design; for instance, a very tiny change in the parameter 'i' from 0.3 to 0.1 mm, which can be a relevant manufacturing tolerance, would lead the antenna resonant frequency to shift down from 2.52 to 2.37 GHz (Fig. 2(b)).

3. Rectifying Circuit and Design

Fig. 3a depicts the rectifier configuration used for converting the RF energy harvested around 2.45 GHz. Even though the antenna is very compact in size, as a showcase, unlike the conventional way of designing the rectifying circuit separately from the antenna part we investigated the integration of the rectifying circuit directly into the antenna terminal, taking benefit from the antenna substrate thickness (Fig. 3b). This has the advantage of placing the rectifying circuit as close as possible to the antenna terminal to minimize the

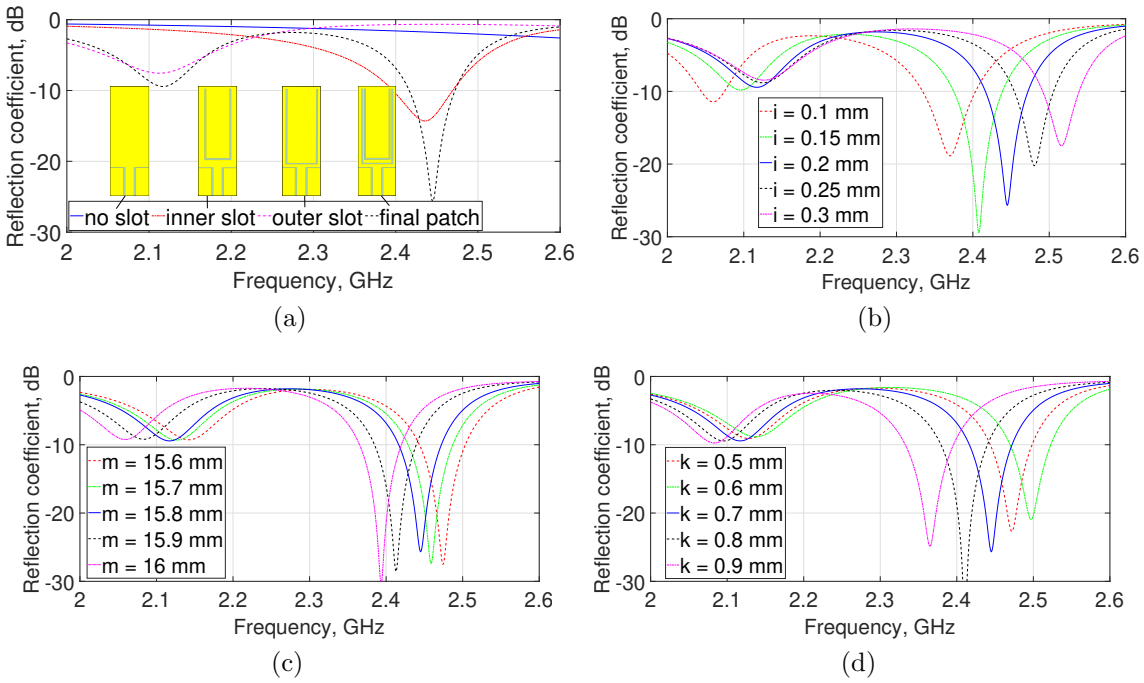

Figure 2: Effects of the antenna key geometrical parameters on its input reflection coefficient: (a) impact of the U-shaped slots on the antenna input reflection coefficient, (b) to (d) antenna input reflection coefficient as a function of antenna parameter 'i', 'm', and k', respectively.

losses and consequently ensure a possibly higher efficiency at low RF power levels. Small pieces of high quality metallic scotch tapes (HB720A [30]) were used at the antenna edge for the circuit layout. This assembly is not fragile, however, to increase its resistivity to external damage, the use of adhesive resin over the soldered components helps improving its stability. Of course, at the expense of a small increase in the antenna size, it is possible to dedicate a small area (roughly around 40 mm^2) of the PCB to lumped elements. Since the proposed rectenna is very compact in size, it provides a degree of freedom for place-and-route even if one wants to consider the rectifying circuit separately from the antenna (see Section 5).

The rectifying circuit was optimized using Keysight Advanced Design System (ADS) software. The rectifier is passive comprising a voltage doubler, a source capacitance of $C_2 = 100$ pF (as RF-pass filter), and a load resistance and capacitance of $R_L = 4.7$ kΩ (to extract DC power) and $C_1 = 100$ pF (as RF-short), respectively. This load resistance was chosen as a representative pressure sensor [31], which is the target application we have in mind for the proposed rectenna. The HSMS-2852 schottky diode (breakdown voltage V_{br}

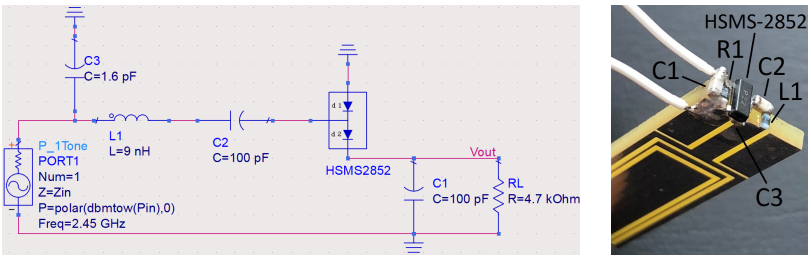

(a) (b)

Figure 3: Rectifier configuration: (a) electrical schematic; (b) photograph of the rectifier integrated with the antenna on its substrate.

= 3.8 V, forward voltage V_{fwd} = 150 mV, and series resistance R_s = 25 Ω) was chosen for rectification due to its relatively low forward bias. To simulate the diode performance in ADS, the non-linear diode model was used [32].

For ambient RF energy harvesting the goal is to have the highest possible PCE at a low input power of typically around −20 to −30 dBm [29, 33]. For maximum power transfer between the antenna and the rectifier, a matching network is necessary. At 2.45 GHz, the designed antenna input impedance (Z_{in}) is 48.3−j6.1 Ω whereas for the diode at an input power (P_{in}) of −20 dBm it is 11−j111.4 Ω (Fig. 4). The maximum variation of the diode input impedance versus P_{in} in the considered frequency range is 30.8% and 2% for real and imaginary part, respectively. A conjugate matching was carried out by using a L-network consisting of a shunt capacitor and a series inductor (Fig. 3a); the optimized values extracted from ADS to have the circuit matched at 2.45 GHz are C_3 = 1.6 pF and L_1 = 9 nH, respectively. Fig. 5 depicts the simulated results of the designed rectifying circuit. A good matching to the antenna (< −20 dB) was achieved, providing a PCE and a DC voltage of 17.7% and 91.2 mV, respectively, at P_{in} = −20 dBm.

Fig. 6 shows PCE results as a function of the load R_L for different input power levels. As observed, at −20 dBm, the PCE reaches its maximum (i.e. 19.1%) for a load value of 8.5 kΩ. The PCE curve is relatively flat around the optimal resistance. Moreover, the proposed rectenna provides PCE results comparable to those previously obtained by rectennas in literature in the same power level range (e.g. [24–28]) but in a much smaller area. In [24]

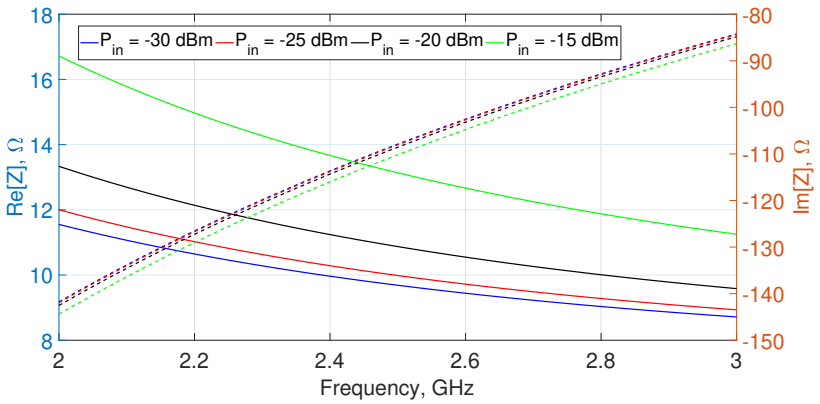

Figure 4: Input impedance of the HSMS-2852 diode for different input power with 4.7 kΩ load and 100 pF shunt capacitor; real part (solid-line), imaginary part (dashed-line).

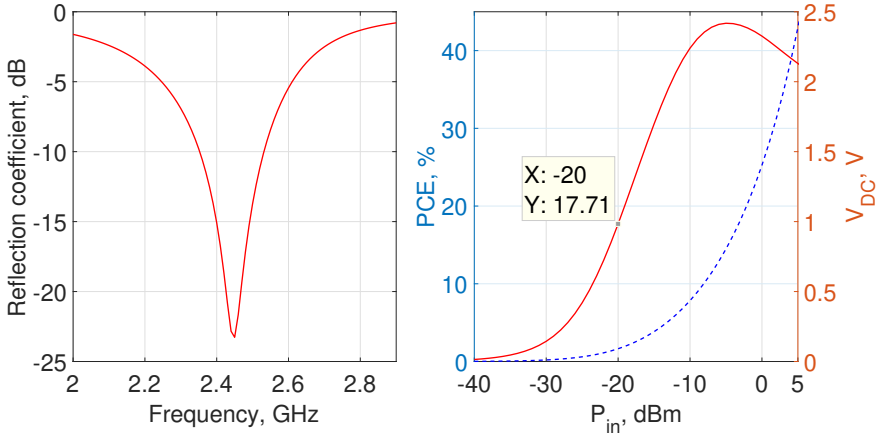

(a) (b)

Figure 5: ADS simulation results of the rectifying circuit with a 4.7 kΩ load: (a) reflection coefficient; (b) PCE and DC output voltage at 2.45 GHz as a function of input power P_{in}.

and [27], for an input power of −10 dBm, efficiencies of 31.9% and 42.1% were reported for 2.1 and 5 kΩ loads, respectively. In our proposed rectenna, with those two loads, the efficiency values are 33.47% and 40.29%, respectively (Fig. 6). In [25] and [28], for $P_{in} = -15$ dBm, the achieved PCE values are 31.8% and 30% with 10 and 2.2 kΩ loads, respectively. In our case, PCE values with those two loads are 29.66% and 24.05%, respectively (Fig. 6). These results confirm that the proposed rectenna is capable of harvesting energy with efficiencies comparable to previously reported harvesters in a significantly reduced area.

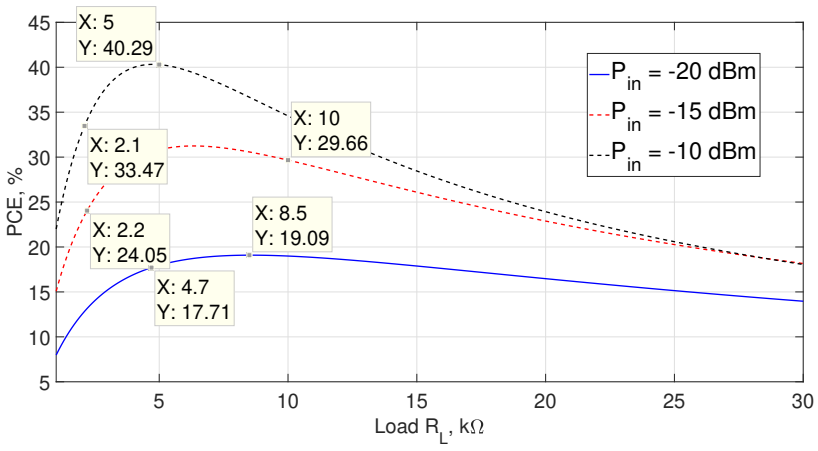

Figure 6: ADS simulation results of PCE as a function of load resistance for different input power levels.

4. Experimental Results and Discussion

In order to validate the proposed rectenna design, experimental results in terms of input reflection coefficient, radiation patterns, peak gain, output DC voltage, and power conversion efficiency are presented. For energy harvesting experiments, a linearly-polarized double-ridged waveguide horn antenna (ETS3115) with a gain of 10 dBi at 2.5 GHz was used to transmit the RF energy generated by an Agilent N9310A signal generator (9 kHz − 3 GHz). The proposed rectenna was placed in front of the transmitter with a large separation distance of 90 cm. A broadband power amplifier (R&K2737M) with maximum 28.9 dB gain was utilized to amplify the RF signal.

The measured and simulated antenna reflection coefficients are presented in Fig. 7. A first look at the results show that, unlike in simulation (solid-blue), the matching level in measurements (dash-back) is weaker in the higher compared to the lower resonant frequency in the band. This is due to the generally known cable influence on electrically small antennas, which lead to inaccurate and unreliable measurements as it changes the antenna structure and current distribution [34]. The good news is that the presence of a cable does not matter for antennas designed for energy harvesting applications as the cable will be replaced by the rectifying circuit. In terms of matching, like in measurement (dash-back), a stronger level in lower frequency than in higher frequency was observed in simulation (solid-red) when a

cable was considered and connected to the antenna (Fig. 7). In that case, there is a tiny frequency shift of 7% between simulation and measurement, which can be attributed to the fabrication imperfection and/or substrate permittivity tolerance. To sum up, the proposed antenna is expected to operate at a center frequency of about 2.45 GHz (with a possible 7% frequency downshift) as there is no cable connection.

The antenna simulated and measured radiation patterns with and without cable are depicted in Fig. 8 both in E- and H-planes at the resonant frequency (x-y and x-z are E- and H-planes, respectively). Although a good agreement between measurement and simulation results was obtained, as electrically small antennas suffer from cable radiation, the disturbance due to the cable is evident (Fig. 8a). The antenna without the cable has a fairly symmetrical radiation pattern in both principal planes (Fig. 8b). The latter monopole-like radiation properties are expected for the proposed rectenna as no cable will be present in the real application as the antenna will be directly connected to the rectifying circuit. In order to be able to calculate the RF-to-DC conversion efficiency in our testbench experiments using Friis equation, the antenna peak gain was measured 0.8 dBi at the resonant frequency, as closely predicted by the full-wave simulations.

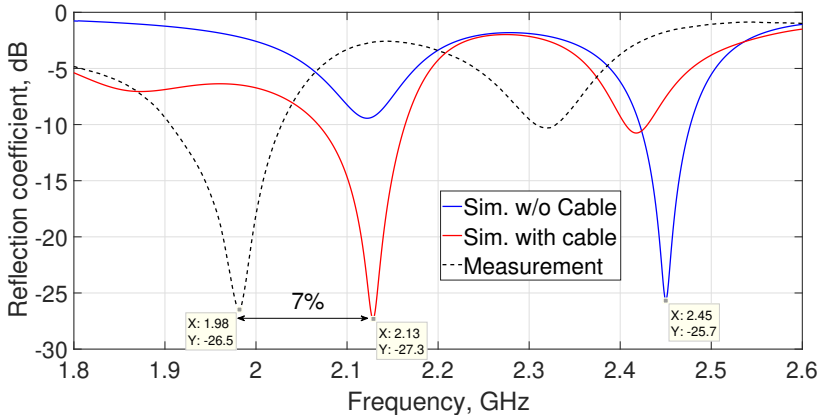

Figure 7: Measured and HFSS simulated input reflection coefficient of the proposed antenna

Fig. 9 illustrates the measured RF-to-DC conversion efficiency and DC output voltage levels at the center frequency of 1.93 GHz with the rectifying circuit layout according to Fig. 3; 1.93 GHz is the frequency where the maximum PCE and V_{DC} were obtained in

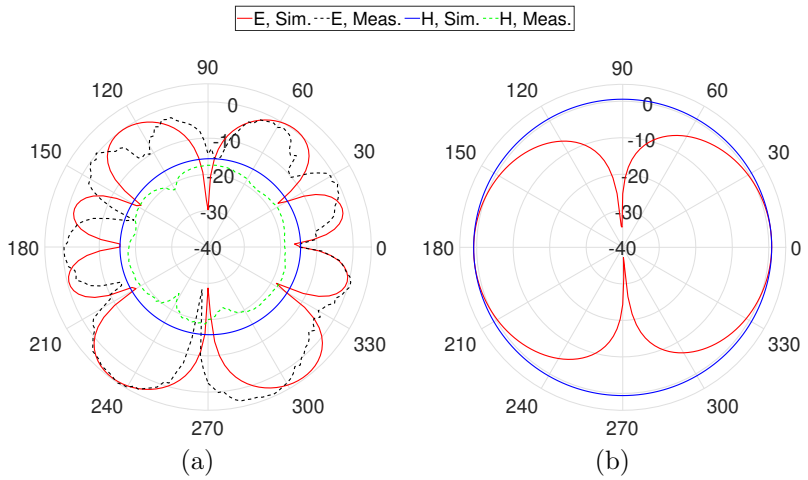

Figure 8: Measured and HFSS simulated radiation patterns at the antenna resonant frequency: (a) with cable, (b) w/o cable (simulation only).

measurement. The simulated results shown in Fig. 9 are with a matching circuit designed to adapt the input impedance of the antenna and the rectifier at 1.93 GHz. This experimental results may arise the following questions: (1) why the antenna without the cable which was supposed to operate at 2.45 GHz is working at 1.93 GHz, and (2) how the matching circuit designed at 2.45 GHz works at 1.93 GHz.

For the first question, a further HFSS simulation was performed with the lumped elements included in the antenna design; results are shown in Fig. 10. Note that a linear model of the schottkey diode, consisting in a resistor ($R_s = 25\ \Omega$) in series with a junction resistance ($R_j \simeq 88\ \Omega$) in parallel with a junction capacitance ($C_j = 0.18$ pF), was considered in HFSS simulation. As observed, in presence of the lumped elements the antenna resonates at 2.08 instead of 2.45 GHz, down-shifted by 15% as a moderate cost for embedding the rectifying circuit in the antenna structure. Taking now into account the 7% frequency shift between measurement and simulation (extracted from input reflection coefficient results), the rectenna operates at a center frequency of 1.93 GHz.

For the second question, as observed in Fig. 10b, the antenna input impedance at 1.93 GHz is 2.61+j15.89 Ω. Based on the ADS simulation, in order to match the latter impedance to the diode impedance (13.8−j148.5 Ω) at 1.93 GHz, the inductor L_1 and the

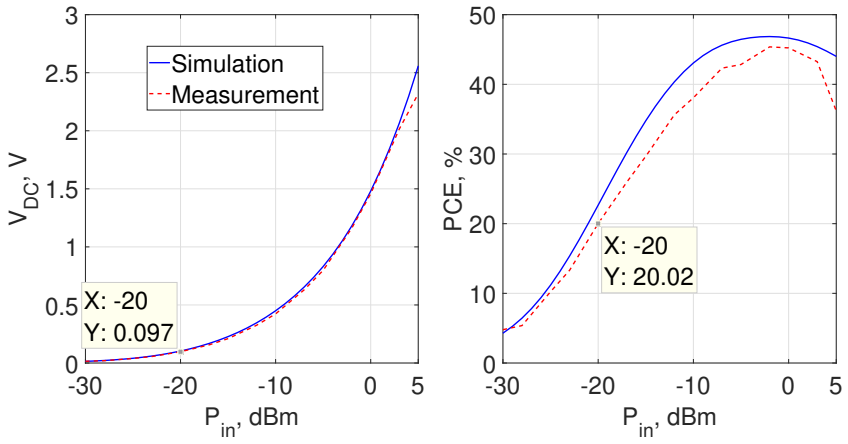

(a) (b)

Figure 9: Measured and ADS simulated RF-to-DC conversion efficiency and output DC voltage at 1.93 GHz: (a) V_{DC}, (b) PCE.

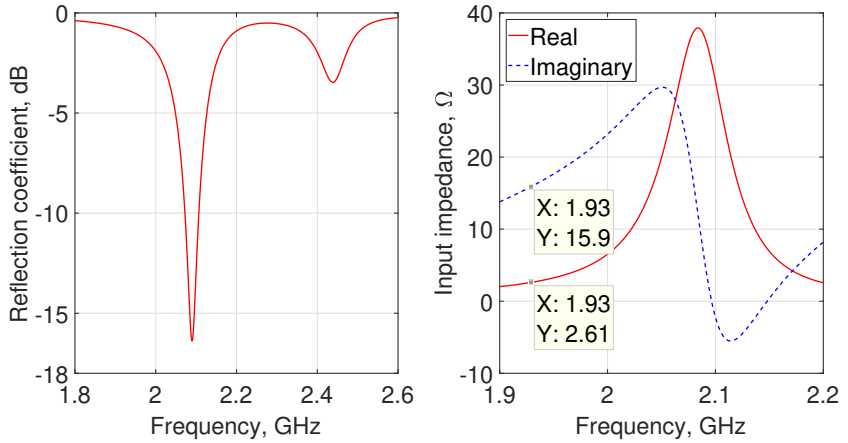

(a) (b)

Figure 10: HFSS simulation results for the antenna with lumped elements included in the design: (a) input reflection coefficient, (b) input impedance.

capacitor C_3 values are to be increased from 9 nH to 9.4 nH and from 1.6 pF tp 3.4 pF. Apart from the manufacturer's lumped-element tolerance values, a very possible reason for the increase of the inductor value in the order of nanoHenry is due to the added inductance by soldering connections [35]. As the capacitor C_3 is mounted between the signal and one of the grounds of the coplanar line (Fig. 3b), it is indeed in parallel with the coupling capacitance between two coplanar conductors and hence leading to increased value (about 1.2 pF according to the formulations provided in [36]).

To sum up, a good agreement between measurement and simulation was obtained. At

an input power of −20 dBm, the maximum PCE and V_{DC} of the proposed rectenna with a 4.7 kΩ load are 20% and 97 mV, respectively. This simple and straightforward energy conversion design can be profitably applied to low-power RF energy harvesting applications, such as radio frequency identification (RFID) and wireless sensor network systems.

5. Experimental Testbench

A demonstration experiment was carried out to show the practical working ability of the designed rectenna (Fig. 11). A primary testbench with the transmitting source setup explained in Section 4 was considered to verify the performance of the rectenna driving a surface mount device (SMD) light-emitting diode LED (Würth elektronik, LED158301260, 3 V threshold voltage) placed 40 cm away from the horn antenna. The choice of 3 V is aimed to emulate future applications requiring energy storage at a voltage high enough to operate RF integrated circuits in short bursts. Due to the strong dependency of the output voltage range of the rectenna on the distance to the input source, a DC-to-DC buck-boost converter (RICOH RP604K331A-TR) with an ultra-low quiescent current (0.3 μA) and a wide input voltage range (1.8 V to 5.5 V) was used to ensure a constant output voltage close to the LED threshold voltage, whatever the voltage across the rectenna. Note that no special effort to redesign the rectifying circuit with respect to the new load (i.e. the buck-boost input impedance, instead of 4.7 kΩ) was made, the main objective being the working ability of the rectenna to wirelessly drive the LED. That explains the limit in measurement distance (no further than 40 cm) in order to compensate for the total available amount of energy and to obtain a voltage at the rectifier output which is high enough to start the buck-boost converter (1.8 V).

As it can be seen in Fig. 11, the rectenna was able to light up the LED at a distance of 40 cm with 10 dBm input power at 2.3 GHz. The led was “ON” with a lower emitting intensity from 2.21 to 2.33 GHz, indicating 12 MHz frequency span, which corresponds to the rectenna operating range. It is worth mentioning that since the rectifying circuit is

Figure 11: Testbench used to characterize the proposed rectenna driving a LED.

printed on a separate PCB, the rectenna operating frequency is close to the one originally designed, i.e. 2.45 GHz, taking into account the 7% frequency downshift extracted from input impedance experiments (more details in Section 4). For a 10 dBm input power and a 26.8 dB power amplifier gain at 2.3 GHz, the power at the horn antenna port was measured 33.4 dBm (due to cable losses) thanks to an Agilent N9320B (9 kHz−3 GHz) spectrum analyzer. The free space path loss for 40 cm at 2.3 GHz is 31.7 dB. Considering 7.9 and 0.8 dBi for the horn and antenna gains, respectively, the power received by the rectenna was almost 10 dBm (10 mW), high enough to ensure a sufficient voltage at the buck-boost output while providing the required output current to visually turn the LED on (minimum 0.25 mA).

It is worth mentioning that for this rectenna configuration with a 4.7 kΩ output resistor at 90 cm separation distance (38.7 dB free space loss), the received power was measured nearly 3 dBm. In that case, the measured DC voltage and current after the rectifier were 2.05 V and 440 μA, respectively. This yields a 0.9 mW DC power and, consequently, a 41.2% RF-to-DC conversion efficiency.

6. Conclusion

Design of a miniaturized printed rectenna was presented for RF power energy harvesting around 2.45 GHz. Its antenna structure consists of a rectangular monopole patch and two U-shaped slots fed by a symmetrical CPW. Even though its antenna is very compact in size, its rectifying circuit was directly attached to the antenna over its substrate only at the expense of

a 15% frequency shift. The overall rectenna dimension is only 24.9 × 8.6 × 1.6 mm^3, which was significantly reduced (by 79%) in comparison to those previously reported for RF energy harvesting applications, while still providing comparable RF-to-DC conversion efficiencies. Experimental results are in a reasonable agreement with the simulated results confirming a good matching level (< -25 dB) and nearly symmetrical radiation patterns (in both E- and H-planes) at the resonant frequency. At a low incident RF power of -20 dBm, the measured maximum RF-to-DC conversion efficiency and DC output voltage of the proposed rectenna are about 20% and 97 mV, respectively, with a load resistance of 4.7 kΩ. The working ability of the proposed rectenna was successfully tested to wirelessly light up a 3 V LED. One perspective would be to store enough energy with a voltage high enough to power sensors and RF emitters for one-way burst data transmission (for example, batteryless, wireless mains switches). In addition to its good performance along with a miniature size, the proposed rectenna offers several mechanical advantages, such as simple structure, light weight, and easy fabrication, which make it a promising candidate for future RF energy harvesting in low-power electronic devices.

Acknowledgements

The authors would like to cordially thank V. Arboux for his assistance with prototype construction.

References

[1] Bizon N., Tabatabaei N.M., Blaabjerg F., Kurt E. Energy harvesting and energy efficiency: technology, methods, and applications, first edition, Springer Int. Publishing, 2017.

[2] Castorina G., Di Donato L., Morabito A.F., Isernia T., Sorbello G. Analysis and design of a concrete embedded antenna for wireless monitoring applications. [An-

tenna Applications Corner]. IEEE Antennas Propag. Magazine. 2016;58:76-93. doi: 10.1109/MAP.2016.2609818.

[3] Adam I., Abd-Malek M.F., Mohd-Yasin M.N., Rahim H.A. Double band microwave rectifier for energy harvesting. Microw. Optical Technol. Lett. 2016;58:922-927. doi: 10.1002/mop.29709.

[4] Valenta C.R., Durgin, G.D. Harvesting wireless power: survey of energy-harvester conversion efficiency in far-field, wireless power transfer systems. IEEE Microwave Magazine. 2014;15:108-120. doi: 10.1109/MMM.2014.2309499.

[5] Tissier J., Latrach M., Popovic Z. 1.84 GHz rectenna optimized by source-pull techniques, for ambient RF energy harvesting applications. URSI Atlantic Radio Science Conf. 2015. Las Palmas, Spain. doi: 10.1109/URSI-AT-RASC.2015.7303007.

[6] Xie F., Yang G., Geyi W. Optimal design of an antenna array for energy harvesting. IEEE Antennas Wirel. Propag. Lett. 2013;12:155-158. doi: 10.1109/LAWP.2013.2243697.

[7] Chou J.H., Lin D.B., Hsiao T.W., Chou H.T. A compact shorted patch rectenna design with harmonic rejection properties for the applications of wireless power transmission. Microw. Optical Technol. Lett. 2016;58:2250-2257. doi: 10.1002/mop.30012.

[8] Chamanian S., Ulusan H., Koyuncuoglu A., Muhtaroglu A., Kulah H. An adaptable interface circuit with multi-stage energy extraction for low power piezoelectric energy harvesting MEMS. IEEE Trans. Power Electronics. 2019;34:2739-2747. doi: 10.1109/TPEL.2018.2841510.

[9] Koohestani M., Golpour M. U-shaped microstrip patch antenna with novel parasitic tuning stubs for ultra wideband applications. IET Microw. Antennas Propag. 2010;4:938-946. doi: 10.1049/iet-map.2009.0049.

[10] Sun X.L., Liu L., Cheung S.W., Yuk T.I. Dual-band antenna with compact radiator for 2.4/5.2/5.8 GHz WLAN applications. IEEE Trans. Antennas Propag. 2012;60:5924-5931. doi: 10.1109/TAP.2012.2211322.

[11] Hua M.J., Wang P., Zheng Y., Yuan S.L. Compact tri-band CPW-fed antenna for WLAN/WiMAX applications. Electron. Lett. 2013;49:1118-1119. doi: 10.1049/el.2013.1669.

[12] Awais Q., Jin Y., Chattha H.T., Jamil M., Qiang H., Khawaja B.A. A compact rectenna system with high conversion efficiency for wireless energy harvesting. IEEE Access. 2018;6:35857-35866. doi: 10.1109/ACCESS.2018.2848907.

[13] Zhang L., Chen B., Jiao Y.C., Weng Z.B. Compact triple-band monopole antenna with two strips for WLAN/WiMAX applications. Microw. Optical Technol Lett. 2012;54:2650-2653.

[14] Kang L., Wang H., Wang X.H., Shi X. Compact ACS-fed monopole antenna with rectangular SRRs for tri-band operation. Electron. Lett. 2014;50:1112-1114. doi: 10.1049/el.2014.1771.

[15] Chen L., Liu Y.F., Ma X.L. Compact ACS-fed circular-arc-shaped stepped monopole antenna for tri-band WLAN/WIMAX applications. Prog. Electromag. Res. C. 2014;51:131-137. doi:10.2528/PIERC14051206.

[16] Kumar A., Naidu P.V., Kumar V., Ramasamy A. Design & development of compact uniplanar semi-hexagonal ACS-fed multi-band antenna for portable system application. Prog. Electromag. Res. M. 2017;60:157-167. doi:10.2528/PIERM17080302.

[17] Haque S.M., Parvez K.M. Slot antenna miniaturization using slit, strip, and loop loading techniques. IEEE Trans. Antennas Propag. 2017;65:2215-2221. doi: 10.1109/TAP.2017.2684191.

[18] Moreira A.A., Pires N., Serro N., Santos R. Ultra wideband dielectric sandwich loaded antennas. 3rd European Conf. Antennas and Propag. 2009, Berlin, Germany.

[19] A. Abbosh, Miniaturization of planar ultrawideband antenna via corrugation. IEEE Antennas Wirel. Propag. Lett. 20108;7:685-688. doi: 10.1109/LAWP.2008.2009323.

[20] Zhang J.W., Huang Y., Cao P. An investigation of wideband rectennas for wireless energy harvesting. Wireless Engineering Technol. 2014;5:107-116. doi: 10.4236/wet.2014.54012

[21] Waterhouse R. Microstrip patch antennas: a designer's guide, Springer Science & Business Media, 2013.

[22] Kang Z., LinX., Tang C., Mei P.,Liu W., Fan Y. 2.45-GHz wideband harmonic rejection rectenna for wireless power transfer. Int. Journal Microw. Wirel. Technol. 2017;9:977-983. doi:10.1017/S1759078716001082.

[23] Yo T.C., Lee C.M., Hsu C.M., Luo C.H. Compact circularly polarized rectenna with unbalanced circular slots. IEEE Trans. Antennas Propag. 2008;56:882-886. doi: 10.1109/TAP.2008.916956.

[24] Shi Y., Fan Y., Jing J., Yang L., Li Y., Wang M. An efficient fractal rectenna for RF energy harvest at 2.45 GHz ISM band. Wiley Int. J. RF Microw. Computer-Aided Engineering. 2018;28:1-8. doi: 10.1002/mmce.21424.

[25] Chen Y., Chiu C. Maximum Achievable Power Conversion Efficiency Obtained Through an Optimized Rectenna Structure for RF Energy Harvesting. IEEE Trans. Antennas Propag. 2017;65:2305-2317. doi: 10.1109/TAP.2017.2682228.

[26] Choi D.Y., Shrestha S., Park J.J., Noh S.K. Design and performance of an efficient rectenna incorporating a fractal structure. Int. J. Commun. Syst. 2014;27:2250-2257.

[27] Vera G.A., Georgiadis A., Collado A., Via S. Design of a 2.45 GHz rectenna for electromagnetic (EM) energy scavenging. IEEE Radio Wirel. Symp. 2010. New Orleans, LA. doi: 10.1109/RWS.2010.5434266.

[28] Ramos I., Popović Z. A compact 2.45 GHz, low power wireless energy harvester with a reflector-backed folded dipole rectenna. IEEE Wireless Power Transfer Conf. 2015. Boulder, CO. doi: 10.1109/WPT.2015.7140159.

[29] Pinuela M., Mitcheson P.D., Lucyszyn S. Ambient RF energy harvesting in urban and semi-urban environments. IEEE Trans. Microw. Theory Techn. 2013;61:2715-2726. doi: 10.1109/TMTT.2013.2262687.

[30] High-quality technical tapes developed for a range of electrical applications. [Online] http://www.hi-bondtapes.com/bondplus-electrical-tapes.

[31] Frank R. Understanding smart sensors. third edition, Norwood, MA: Artech House, 2013.

[32] Agilent Technologies Application Note 1156, Diode detector simulation using Agilent technologies EEsof ADS Software.

[33] Andrenko A.S., Lin X., Zeng M. Outdoor RF spectral survey: A roadmap for ambient RF energy harvesting. TENCON 2015 - 2015 IEEE Region 10 Conference, Macao, 2015. doi: 10.1109/TENCON.2015.7373140.

[34] Hirasawa K., Haneishi M. Analysis, design, and measurement of small and low-profile antennas. Boston, MA: Artech House, 1992.

[35] Dally W.G., Poulton J.W. Digital Systems Engineering. first edition, Cambridge University Press. 1998. doi:10.1017/CBO9781139166980.

[36] Clayton R.P. Analysis of multiconductor transmission lines. second edition, Hoboken, New Jersey, John Wiley & Sons - IEEE Press, 2008.